

# The Pallbearer E3 Ligase Promotes Actin Remodeling via RAC in Efferocytosis by Degrading the Ribosomal Protein S6

Hui Xiao,<sup>1,5</sup> Hui Wang,<sup>1,6</sup> Elizabeth A. Silva,<sup>2,7</sup> James Thompson,<sup>3</sup> Aurélien Guillou,<sup>4</sup> John R. Yates, Jr. III,<sup>3</sup> Nicolas Buchon,<sup>4</sup> and Nathalie C. Franc<sup>1,2,\*</sup>

<sup>1</sup>Department of Immunology and Microbial Science and Department of Cell and Molecular Biology, The Scripps Research Institute, La Jolla, CA 92037, USA

<sup>2</sup>Medical Research Council Laboratory for Molecular Cell Biology, London WC1E 6BT, UK

<sup>3</sup>Department of Chemical Physiology, The Scripps Research Institute, La Jolla, CA 92037, USA

<sup>4</sup>Department of Entomology, Cornell University, Ithaca, NY 14853, USA

<sup>5</sup>Present address: Department of Developmental Neurobiology, St. Jude Children's Research Hospital, Memphis, TN 38105, USA

<sup>6</sup>Present address: Department of Pathology, Hebei Medical School, Shijiazhuang City 050017, China

<sup>7</sup>Present address: University of California San Francisco, San Francisco, CA 94158, USA

\*Correspondence: [nfranc@scripps.edu](mailto:nfranc@scripps.edu)

<http://dx.doi.org/10.1016/j.devcel.2014.11.015>

## SUMMARY

Clearance of apoptotic cells (efferocytosis) is achieved through phagocytosis by professional or amateur phagocytes. It is critical for tissue homeostasis and remodeling in all animals. Failure in this process can contribute to the development of inflammatory autoimmune or neurodegenerative diseases. We found previously that the PALL-SCF E3-ubiquitin ligase complex promotes apoptotic cell clearance, but it remained unclear how it did so. Here we show that the F-box protein PALL interacts with phosphorylated ribosomal protein S6 (RpS6) to promote its ubiquitylation and proteasomal degradation. This leads to RAC2 GTPase upregulation and activation and F-actin remodeling that promotes efferocytosis. We further show that the specific role of PALL in efferocytosis is driven by its apoptotic cell-induced nuclear export. Finding a role for RpS6 in the negative regulation of efferocytosis provides the opportunity to develop new strategies to regulate this process.

## INTRODUCTION

Innate immunity is the first line of host defense of all animals. It limits infection by clearing pathogens (Modlin, 2012). Humoral responses in innate immunity have been studied extensively (Shishido et al., 2012), but its cellular responses are still poorly understood. This includes phagocytosis, the process by which specialized cells, the phagocytes, recognize, engulf, and digest pathogens, tissue debris, and necrotic cells during infection and in wound healing (Brown, 1995). Phagocytosis is also critical for tissue homeostasis because approximately 50–70 billion of our cells die daily by apoptosis (Han and Ravichandran, 2011). Professional and amateur phagocytes rapidly clear these

apoptotic cells (ACs), a process known as efferocytosis (Henson et al., 2001). Failure to clear ACs can promote neurodegeneration and autoimmunity (Fuller and Van Eldik, 2008; Muñoz et al., 2010). It has also been associated with age-related macular retinal degeneration and with systemic lupus erythematosus (Finnemann et al., 2002; Hanayama et al., 2006). A thorough understanding of phagocytosis is essential to design new drugs to fight infection and to prevent and/or treat neurodegenerative and autoimmune diseases.

*Drosophila* is an ideal model organism in which to study innate immune responses, including phagocytosis (Ferrandon et al., 2007). It has macrophage-like cells (Tepass et al., 1994), and *Drosophila* Schneider S2 cells behave like macrophages and are amenable to RNAi and biochemistry (Schneider, 1972). Using genetic and genome-wide RNAi screens, we previously identified several molecules required for efferocytosis, including Pallbearer (PALL), an F-box protein that acts within a SkpA/dCullin-1/F-box (SCF) complex (Silva et al., 2007). This PALL-SCF complex functions as an E3-ubiquitin ligase to promote efficient AC clearance (Silva et al., 2007).

E3-ubiquitin ligases are involved in a variety of biological processes where the F-box protein is generally responsible for the binding specificity of the substrate to be degraded via the proteasome (Deshaies, 1999). Many F-box proteins have specific protein-protein interaction domains, such as leucine-rich repeats, WD-40 repeats, Sec7, or others, that have facilitated the identification of their substrate(s). However, many other F-box proteins do not have such domains, making it more difficult to identify their substrates. PALL belongs to this subclass, and what its substrate(s) for degradation may be in efferocytosis is not yet known.

Here we used both biochemistry and genetics to find the PALL substrate(s). We show that PALL interacts with the ribosomal protein S6 (RpS6) and that this interaction depends on the phosphorylation of RpS6. Treatment of S2 cells with the proteasome inhibitor MG132 results in accumulation of polyubiquitylated RpS6, revealing a role for the ubiquitin-proteasome pathway in the regulation of RpS6 levels. The polyubiquitylation and degradation of RpS6 are PALL-dependent because we

observed less polyubiquitylated forms of RpS6 in *pall* RNAi-treated S2 cells. RNAi of *RpS6* enhances AC engulfment in S2 cells, and, conversely, overexpressing RpS6 in embryonic macrophages partially inhibits AC clearance in vivo. Mutation of *RpS6* suppresses the AC clearance defect phenotype of a *pall* mutant allele. We found that *pall* and *RpS6* mutant macrophages have opposite F-actin phenotypes, with F-actin accumulation in *pall* mutants and diminished F-actin in *RpS6* mutants. Also, *pall* and *RpS6* RNAi-treated S2 cells have opposite staining phenotypes for RAC. RAC regulates actin cytoskeleton during AC clearance in *Caenorhabditis elegans* and mammalian systems (Gumienny et al., 2001; Kinchen et al., 2005), and RAC2 is required for efferocytosis in *Drosophila* S2 cells (Cuttell et al., 2008). Cells treated with *pall* RNAi have less total and active RAC2, whereas *RpS6* RNAi-treated S2 cells have more. Importantly, overexpressing RAC2 in *pall* mutant macrophages rescued their phagocytosis defect. Therefore, we propose that the PALL/SCF complex promotes the proteasomal degradation of RpS6, which acts as a negative regulator of efferocytosis. This degradation leads to F-actin cytoskeleton remodeling via the upregulation and activation of RAC2, thereby promoting phagocytosis. Finally, we show that PALL is not required for phagocytosis of bacteria and that its specificity in efferocytosis is driven by its AC-induced nuclear export.

## RESULTS

### PALL Physically Interacts with RpS6

We proposed previously that PALL promotes efferocytosis by promoting ubiquitylation and proteasomal degradation of one or more phosphorylated substrates (Silva et al., 2007). To identify the PALL substrate(s), we established three stable S2 cell lines that express hemagglutinin (HA)-tagged, full-length PALL (HA-PALLFL), its F-box-deleted version (HA-PALLΔF), or the F-box protein SLIMB (HA-SLIMB), which plays a role in innate immunity but not in efferocytosis (Khush et al., 2002; Silva et al., 2007). We used protein extracts of these stable cell lines in immunoprecipitations (IPs) with HA antibody (Ab) and carried out comparative analyses of the IPs on SDS-PAGE. We found one endogenous protein of around 26 kDa in coimmunoprecipitations with both HA-PALLFL and HA-PALLΔF but not with HA-SLIMB. Using MALDI-TOF mass spectrometry (MS), we identified this interactor as the ribosomal protein S6 (RpS6), a component of the 40S subunit of the ribosome (Figure 1A). Although ribosomal proteins are abundant and often pulled nonspecifically in IPs, RpS6 was the only ribosomal protein being consistently pulled down with HA-PALLFL and HA-PALLΔF, but not with HA-SLIMB, in three other independent IPs subjected to comparative tandem MS (Figure 1B). RpS6 sequences recovered in the MS are indicated in blue in Figure 1C. Treatment of S2 cells with cycloheximide, an inhibitor of protein translation, did not significantly enhance or reduce the ability of S2 cells to clear ACs, arguing that the role of RpS6 in efferocytosis is independent of its role as a component of the small ribosomal subunit in the context of protein synthesis (Figure S1A available online). Deleting the F-box domain of PALL prevents its interaction with SkpA (Silva et al., 2007; Figure 1D), eliminating the possibility that RpS6 is binding to the other components of the PALL-SCF complex. We further confirmed the interaction between PALL and RpS6 in cotrans-

fections in S2 cells using HA-PALLFL- and RpS6-FLAG-tagged constructs (Figure 1D) as well as HA-PALLFL-, HA-PALLΔF-, and RpS6-V5-tagged constructs (Figure 1E; Figure S1B). Therefore, *RpS6* interacts with PALL and is a candidate substrate of PALL.

### RpS6 Phosphorylation Is Required for Its Interaction with PALL

RpS6 is a component of the 40S subunit of the ribosome and the substrate of several mammalian serine/threonine protein kinases that can phosphorylate RpS6 at S233, S235, S239, S242, and S245 (S indicated in red in Figure 1C), all of which are highly conserved (Radimerski et al., 2000). One of the RpS6 peptide identified by MS included a carboxy-terminal peptide that contains the conserved serines, as highlighted in blue in Figure 1C. Substrates of F-box proteins are generally phosphorylated prior to specifically interacting with their respective F-box proteins. To address whether RpS6 phosphorylation at its conserved serines is a prerequisite for its interaction with PALL, we generated a V5-tagged mutated construct of RpS6 under the control of the metallothionin (MT)-inducible promoter where all five serines were mutated into alanines (*MT-RpS6(S/A)-V5*). We cotransfected this construct into S2 cells with either HA-PALLFL and HA-PALLΔF constructs, carried out IPs with HA Ab, and probed for RpS6(S/A)-V5 using V5 Ab on western blots (WBs). RpS6(S/A)-V5 could no longer coimmunoprecipitate with either HA-PALLFL or HA-PALLΔF (Figure 1E). Therefore, serine phosphorylation of RpS6 is required for its interaction with PALL.

### PALL Promotes Polyubiquitylation and Proteasomal Degradation of RpS6

The interaction of phosphorylated RpS6 with PALL suggests that RpS6 is a target of the PALL-SCF complex for polyubiquitylation and proteasomal degradation. This hypothesis was further strengthened by our observation that the input level of expression of the mutated form of RpS6, RpS6(S/A)-V5, in S2 cells was greater than that of RpS6-V5 under similar cotransfection conditions as well as in the sole presence of endogenous PALL (see V5 input in Figure 1E). This result suggests that mutating the serine phosphorylation sites of RpS6 into alanines, which abolishes RpS6 interaction with PALL, prevents its ubiquitylation and degradation via the proteasome. To test this, we asked whether RpS6 could accumulate when inhibiting the proteasome. We overexpressed RpS6-V5 in HA-PALLFL-stable S2 cells in the presence or absence of the proteasome inhibitor MG132 and quantified the level of RpS6 protein in WBs. RpS6-V5 accumulated in the presence of MG132 (Figure 2A) because its expression level increased significantly by  $34.2\% \pm 17.1\%$  ( $p < 0.05$ ) when compared with that in the absence of MG132 (Figure 2B). We could not evaluate the levels of phosphorylated RpS6 because commercial antibodies against mammalian phosphorylated RpS6 do not cross-react with *Drosophila* RpS6.

To further address whether RpS6 is a substrate of PALL-SCF for ubiquitylation, we overexpressed RpS6-V5 with an Act5C-ubiquitin (Act5C-Ub) construct in HA-PALLFL-stable S2 cells in the presence or absence of the proteasome inhibitor MG132. We immunoprecipitated RpS6-V5 with V5 Ab and performed a

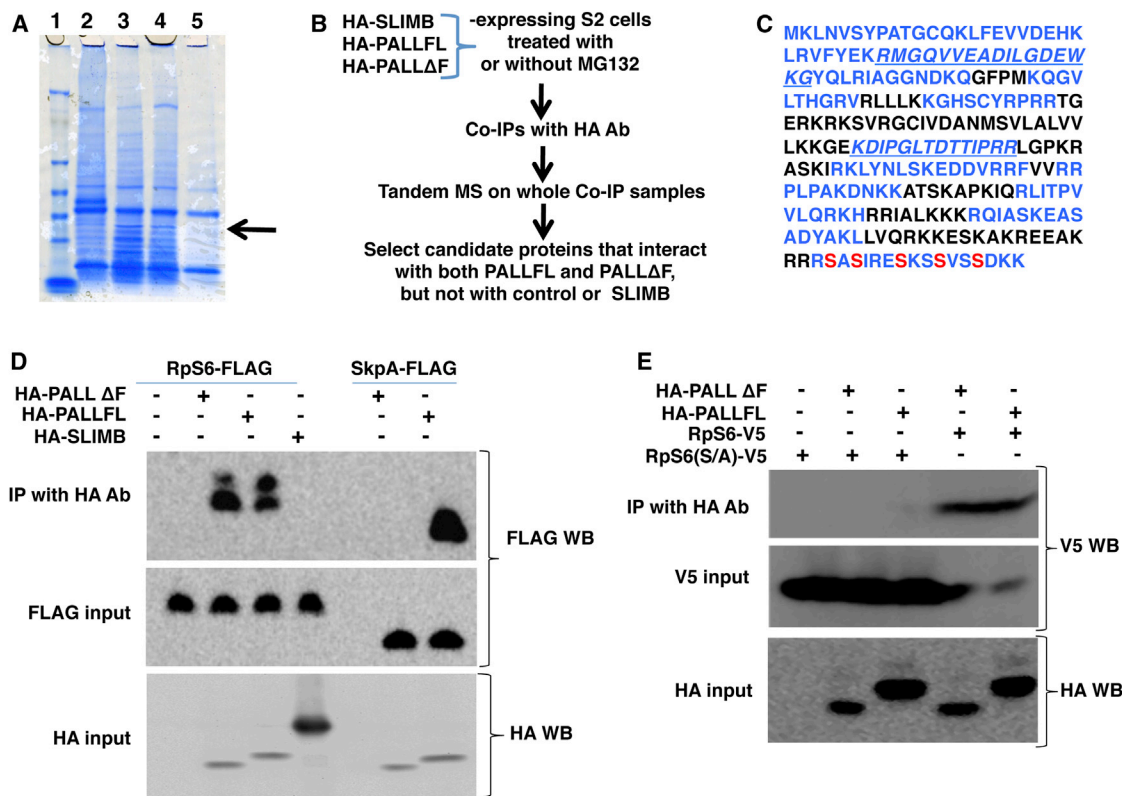


### Figure 1. PALL Physically Interacts with Phosphorylated Rps6

(A) SDS-PAGE and Coomassie blue staining of HA Ab immunoprecipitates of HA-PALLFL-, HA-PALLΔF-, or HA-SLIMB-expressing S2 cell extracts. RpS6 is identified by differential band cutout, and MALDI-TOF is indicated by an arrow. Lane 1, protein ladder; lane 2, HA-SLIMB (unrelated F box); lane 3, HA-PALLFL; lane 4, HA-PALLΔF (F box-deleted PALL); lane 5, control S2 cells.

(B) Flow chart of IPs and tandem MS with HA-SLIMB (control irrelevant F-box protein), HA-PALLFL, and HA-PALLΔF (F-box-deleted PALL) stable S2 cells.

(C) Primary amino acid sequence of endogenous RpS6. In blue are sequences found by tandem MS. Phosphorylated serines are indicated in red.

(D) IPs with HA Ab of crude protein extracts from transiently transfected S2 cells expressing RpS6-FLAG or SkpA-FLAG and HA-SLIMB, HA-PALLFL, or HA-PALLΔF. Shown are RpS6-FLAG immunoprecipitates with HA-PALLFL and HA-PALLΔF but not with HA-SLIMB. As a control, SkpA-FLAG immunoprecipitates with HA-PALLFL but not HA-PALLΔF. Inputs are given by WB detection on protein extracts of RpS6-FLAG and SkpA-FLAG or of HA-SLIMB-, HA-PALLFL-, and HA-PALLΔF-expressing cells with FLAG and HA Abs, respectively (see also Figure S1B).

(E) IPs with HA Ab of protein extracts from S2 cells expressing RpS6-V5 or its RpS6(S/A)-V5 mutant with HA-PALLFL or HA-PALLΔF, followed by V5 Ab WB. The PALL/RpS6 interaction is lost when RpS6 is mutated at its serine phosphorylation sites.

See also Figure S1.

WB with ubiquitin (Ub) Ab to assess whether RpS6 could be ubiquitylated (Figure 2C). We detected several polyubiquitylated forms of RpS6 in the presence of MG132 but not in its absence (Figure 2C). These results demonstrate conclusively that RpS6 is a substrate for polyubiquitylation.

We then asked whether ubiquitylation of RpS6 was PALL-dependent. For this, we repeated the above experiments in *pall* RNAi-treated S2 cells in the presence of MG132. We found that the level of detectable polyubiquitylated RpS6 was reduced by almost 55% when compared with MG132-treated control S2 cells (Figures 2D and 2E). As in Figure 2A, the level of RpS6-V5 expression was higher in MG132-treated cells than in untreated control S2 cells (see V5 input WB in Figure 2D). Together, these results demonstrate a previously unappreciated role for the ubiquitin-proteasome pathway in the regulation of RpS6 protein levels. Therefore, PALL is required for the specific interaction of RpS6 with the PALL-SCF complex and subsequent RpS6 polyubiquitylation and proteasomal degradation.

### An RpS6 Loss-of-Function Mutation Suppresses the Loss-of-Function Phenotype of *pall*

To further assess whether RpS6 acts as a substrate for polyubiquitylation and proteasomal degradation via the PALL-SCF complex in vivo, we asked whether *RpS6* and *pall* might interact genetically. Because a loss of function of *pall* is expected to result in RpS6 accumulation, we asked whether a loss of function of *RpS6* might suppress the loss-of-function phenotype of *pall*, i.e., restore AC clearance in the *pall*-null allele. Previously characterized *pall* alleles were not single mutants of *pall* but also affected neighboring genes (Silva et al., 2007). Therefore, we generated a *pall*<sup>ko</sup>-null allele by homologous recombination (Figures S2A–S2B). As anticipated, *pall*<sup>ko</sup> macrophages have a defect in phagocytosis of ACs in vivo when compared with wild-type macrophages (Figure S2C). Of note is that *pall*<sup>ko</sup> does not appear to have any obvious growth-related phenotypes at any developmental stages. Although we did not look extensively for these types of phenotypes at the cellular level, the

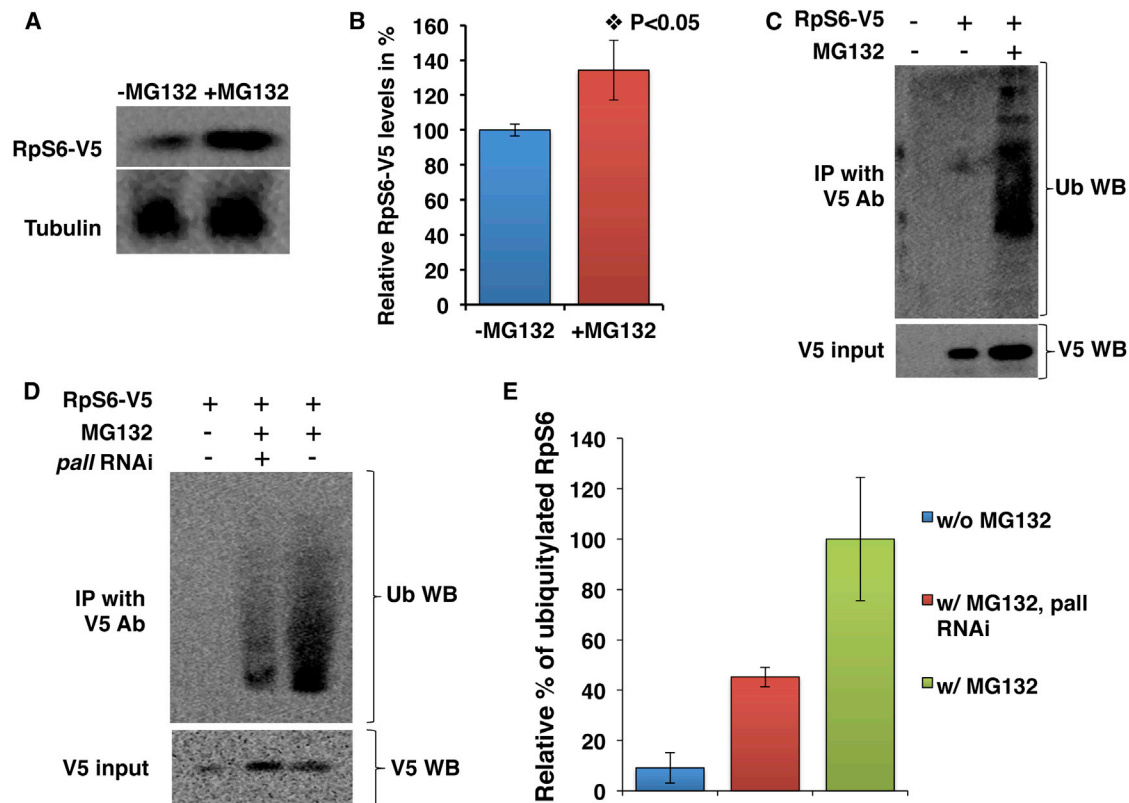


**Figure 2. Rps6 is a Substrate of PALL for Polyubiquitylation and Proteasomal Degradation**

(A) HA-PALLFL stable S2 cells transfected with Rps6-V5 and treated with or without MG132, followed by WB with V5 Ab. The tubulin WB served as a loading control.

(B) Graph summarizing the quantification of (A). Bars represent the relative percentage when compared with untreated (–MG132) cells  $\pm$  SEM of three independent experiments.

(C) HA-PALLFL stable S2 cells transfected with Rps6-V5 and Act5C-Ub constructs and treated with or without MG132. V5 Ab immunoprecipitates of Rps6 were blotted with Ub Ab to detect polyubiquitylated forms of Rps6. The input of Rps6-V5 protein is shown by WB of crude cell extracts with V5 Ab.

(D) The same experiments as in (C) but with or without pretreating the S2 cells with *pall* RNAi prior to MG132 treatment and IP with V5 Ab and WB with Ub Ab. The input of Rps6-V5 protein is shown by WB of crude cell extracts with V5 Ab.

(E) Graph showing the relative quantification of the mean percent  $\pm$  SEM of ubiquitylated Rps6 in S2 cells without MG132 (w/o MG132) and *pall*-RNAi cells in the presence of MG132 (w/MG132 *pall* RNAi) compared with control S2 cells with MG132 (w/MG132).

phosphorylation of Rps6 in the context of efferocytosis is also independent of the target of rapamycin (TOR) and S6 kinase pathway (H.X. and N.C.F., unpublished data).

We then crossed our *pall*<sup>ko</sup> to a previously characterized strong hypomorphic loss-of-function allele of Rps6, *Rps6*<sup>WG1288</sup> (Watson et al., 1992), and assessed the phagocytosis phenotypes and phagocytic indices (PIs) of homozygous *pall*<sup>ko</sup> macrophages that were either heterozygous or homozygous for *Rps6*<sup>WG1288</sup> by CRQ Ab and 7-amino actinomycin-D (7-AAD) double staining and confocal microscopy (Silva et al., 2007; Figure 3). Double-homozygous mutant macrophages were capable of engulfing ACs (Figure 3C) with a PI of  $2.61 \pm 0.28$ , similar to that of control macrophages (Figure 3D) and of *Rps6*<sup>WG1288</sup> homozygous macrophages (Figure 3A) with PIs of  $2.47 \pm 0.16$  and  $2.4 \pm 0.22$ , respectively (Figure 3D) ( $p > 0.05$ ). Therefore, loss of function of *Rps6* rescued the phagocytosis phenotype defect of homozygous *pall*<sup>ko</sup> mutant macrophages, which had a PI of  $1.35 \pm 0.12$ , whereas mutating one copy of *Rps6* did not significantly affect the homozygous *pall*<sup>ko</sup> mutant pheno-

type (Figures 3B and 3D) ( $p < 0.05$  compared with control, and  $p > 0.05$  when compared with *pall*<sup>ko</sup>). Together, these results demonstrate that *Rps6* and *pall* interact genetically and act in the same pathway in vivo, where *Rps6* acts downstream of *pall* as its substrate for polyubiquitylation and proteasomal degradation.

### Rps6 Acts as a Negative Regulator of Efferocytosis

Rps6 is a substrate of PALL for proteasomal degradation to promote AC clearance, therefore arguing that Rps6 acts in macrophages as a negative regulator of this process. In a genome-wide RNAi screen for genes required in AC clearance in S2 cells, we found that *Rps6* RNAi treatment of S2 cells with both DRSC18712 and DRSC25010 could enhance phagocytosis of ACs (<http://www.flyrnai.org>; Figure 4). Compared with mock-treated S2 cells (Figure 4A), *Rps6* RNAi-treated S2 cells with DRSC25010 were more than 2-fold more phagocytic when given a same amount of ACs (Figures 4C and 4G). RNAi-treatments of two other components of the small ribosome subunit, such as

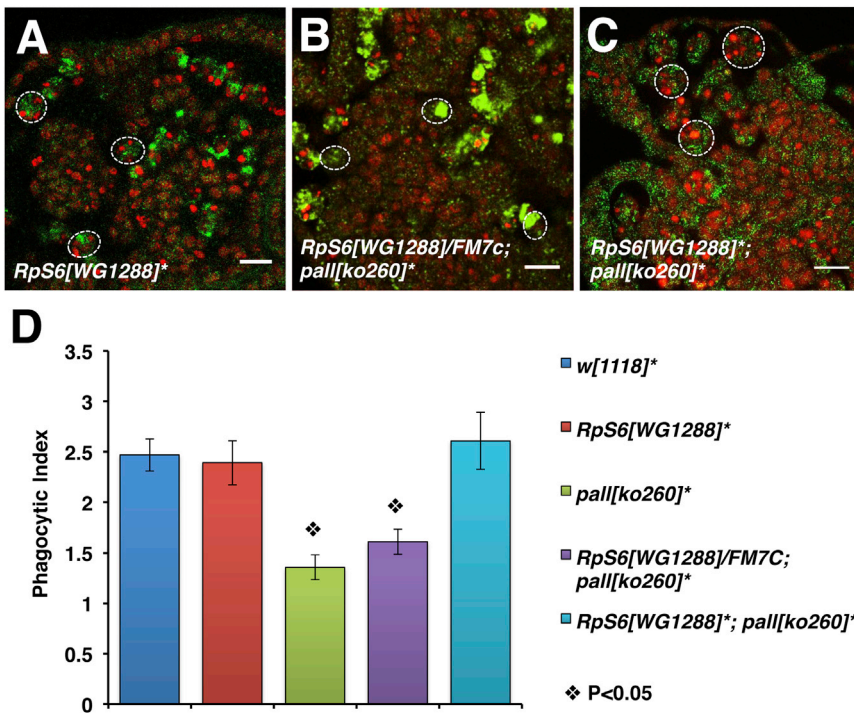


**Figure 3. A Loss-of-Function Mutation of *RpS6* Suppresses the Loss-of-Function Mutation Phenotype of *pall* In Vivo**

(A–C) Confocal micrographs of *RpS6*<sup>WG1288</sup> homozygous embryos, *RpS6*<sup>WG1288</sup>/+; *pall*<sup>ko260</sup>/*pall*<sup>ko260</sup> embryos, and *RpS6*<sup>WG1288</sup>; *pall*<sup>ko260</sup> double-homozygous embryos stained with the CRQ Ab (green) and 7-AAD (red). Dotted white circles outline single macrophages. Scale bars, 10  $\mu$ m.

(D) Graph showing the mean Pls  $\pm$  SEM for each genotype. \*, homozygous alleles.

See also Figure S2.

*RpS10b* (the knockdown of which enhances phagocytosis of *Listeria monocytogenes* [Agaïsse et al., 2005]) and *RpS2*, served as controls and did not significantly affect the ability of S2 cells to engulf ACs (Figures S3A and S3B).

We further tested whether *RpS6* could act as an inhibitor of efferocytosis in vivo by driving the expression of two independent *UAS-RpS6* transgenic lines under the control of the macrophage-specific *crq-Gal4* transgene (Figures 4D–4F and 4H). Overexpressing *RpS6* with either *UAS-RpS6* lines resulted in a >30% decrease in phagocytosis by embryonic macrophages in vivo (compare Figures 4E and 4F with Figure 4D), with Pls of  $2.36 \pm 0.27$  and  $2.32 \pm 0.31$  versus  $3.44 \pm 0.47$  in the *crq-gal4* control ( $p < 0.05$ ) (Figure 4H). The macrophage-specific overexpression of other components of the small ribosome subunits, including *RpS2* and *RpS10b*, did not affect their phagocytic ability (Figure S3C). Therefore, *RpS6* acts as a negative regulator of efferocytosis, which further fits with its role as a PALL substrate for polyubiquitylation and proteasomal degradation, thereby promoting efficient engulfment of ACs. Furthermore, this role for *RpS6* appears to be independent of its ribosomal function.

### PALL and *RpS6* Regulate F-Actin Cytoskeleton Rearrangement in Efferocytosis

How do PALL and *RpS6* act in regulating AC clearance? F-actin cytoskeleton rearrangement is an important hallmark of phagocytosis (Allen and Aderem, 1996). Recently, phosphorylated *RpS6* was attributed a role in regulating F-actin organization and junctional protein recruitment at the blood-testis barrier during spermatogenesis, where increased level of phosphorylated *RpS6* disrupted the barrier and colocalized with disorganized F-actin (Mok et al., 2012). Therefore, we next asked whether *pall* facilitates AC clearance by promoting *RpS6* polyubiquityla-

tion and degradation and subsequent F-actin remodeling. We first assessed the F-actin phenotype of mock- and *pall* RNAi-treated S2 cells (Figures S4A and S4B, respectively) by phalloidin staining. The F-actin immunostaining increased by  $73\% \pm 6.4\%$  in *pall* RNAi-treated S2 cells compared with the mock-treated cells (Figure S4C). The *pall* mRNA expression was down by about 75% in *pall* RNAi-treated S2 cells compared with mock-treated cells (Figure S4D). To find out whether *pall* regulates F-actin in vivo, we further assessed the actin phenotype of *pall*<sup>ko</sup> macrophages. As for Phalloidin staining in *pall* RNAi-treated S2 cells, F-actin immunostaining increased in *pall*<sup>ko</sup> macrophages (Figure 5B) compared with that of wild-type macrophages (Figure 5A). In contrast, F-actin immunostaining was weaker in *RpS6*<sup>WG1288</sup> mutant macrophages (Figure 5C) compared with wild-type macrophages (Figure 5A), therefore having the anticipated opposite phenotype. Similar results were obtained with phalloidin staining of *pall* and *RpS6* mutant macrophages in vivo (data not shown). These data argue that PALL and *RpS6* play a role in regulating the F-actin cytoskeleton in *Drosophila* macrophages in vivo. Furthermore, *pall* RNAi-treated S2 cells were more rounded than mock-treated cells, with F-actin distributed evenly around their cell cortex, whereas F-actin staining was weaker in *RpS6*-RNAi cells and more localized at their basal membrane (i.e., at their point of contact with the glass slide) (Figures 5D and 5E). *RpS6* RNAi-treated cells spread onto glass slides and made more membrane ruffles than mock-treated cells (Figures 5D and 5E). Tubulin and actin monomers expression levels in *pall*- or *RpS6*- RNAi cells were comparable with that of mock-treated cells (Figure 6A). Therefore, PALL and *RpS6* regulate F-actin cytoskeleton rearrangement in vivo and in S2 cells.

### PALL and *RpS6* Regulate the *Drosophila* RAC2 Level and Activity in Efferocytosis

The small GTPase RAC has been shown to play an important role in AC clearance in both *C. elegans* and mammalian systems (Gumienny et al., 2001; Kinchen et al., 2005) by promoting actin remodeling. In a genome-wide RNAi screen for genes required for AC clearance by S2 cells, we found a role for the small GTPase RAC2 but not for the other RAC family members,

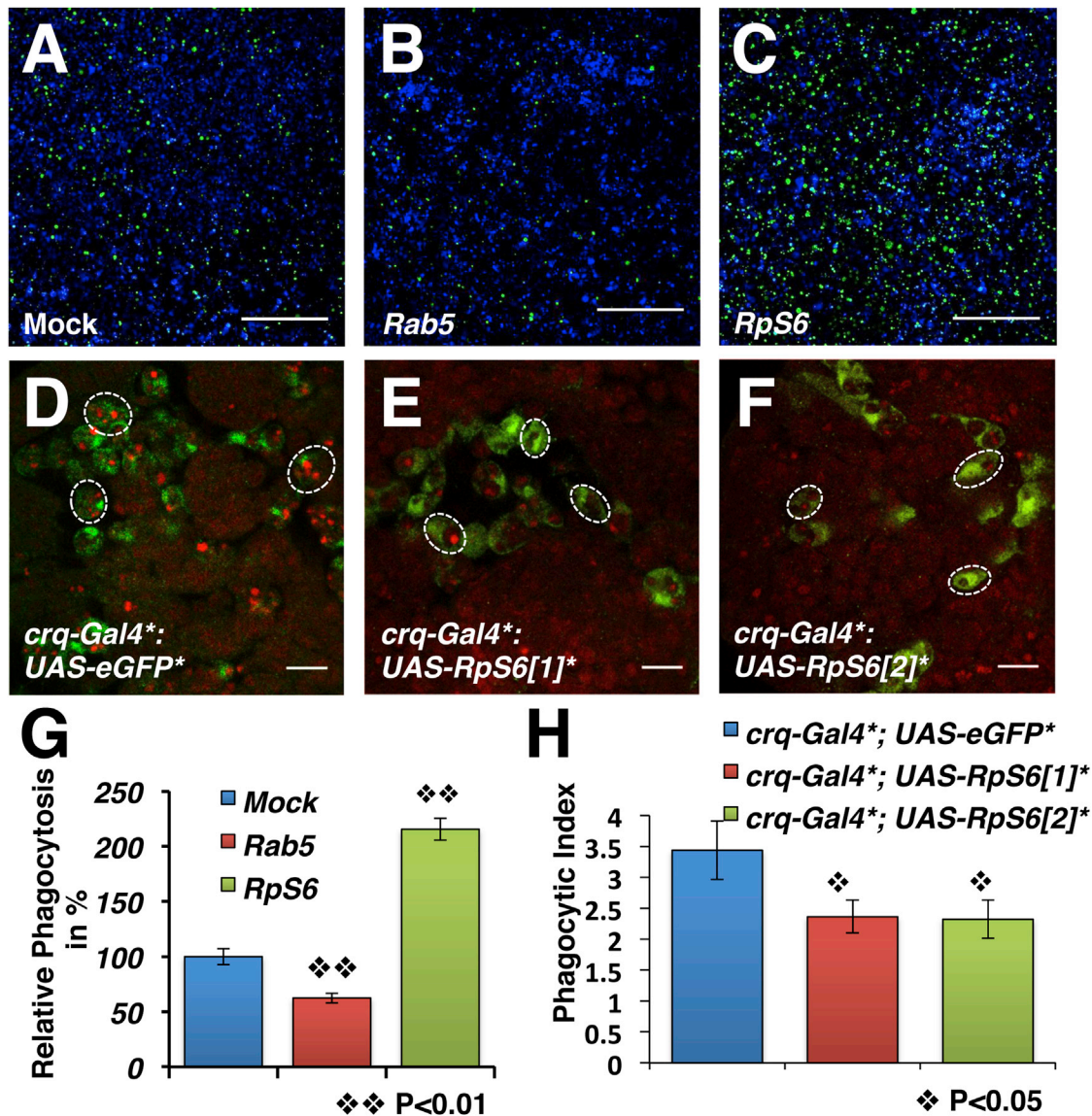


**Figure 4. *RpS6* Acts as a Negative Regulator of AC Clearance**

(A–C) Phagocytosis of ACs by mock-treated (A), *Rab5* RNAi-treated (B), or *RpS6* RNAi-treated (C) S2 cells. Live cells are blue, and engulfed FITC-labeled ACs are green. Scale bars, 200  $\mu$ m.

(D–F) Merged confocal images of *yw*; +; *crq-Gal4*, *UAS-eGFP* (wild-type reference) (D) and *yw*; *UAS-RpS6*; *crq-Gal4*, *UAS-eGFP* macrophages with two independent transgenic *UAS-RpS6* lines, [1] and [2], in (E) and (F), respectively. ACs are stained with 7-AAD (red), and GFP-expressing macrophages appear green. Scale bars, 10  $\mu$ m.

(G) Graph summarizing the quantification of (A–C) with *rab5*-RNAi S2 cells as a control. Bars represent the relative phagocytosis compared with mock-treated S2 cells  $\pm$  SEM of three independent experiments with duplicated wells.

(H) Graph showing the mean PIs  $\pm$  SEM for each genotype in (D–F).

See also Figure S3.

RAC1 and MTL (Mig-2 like) (Cuttell et al., 2008). We asked whether PALL and *RpS6* might regulate RAC levels and/or activity in S2 cells. On a WB of total protein extracts from RNAi-treated S2 cells, we observed that there was approximately 57% less and 40% more total RAC in *pall* RNAi and *RpS6* RNAi cells, respectively, than in mock-treated cells (Figures 6A and 6B). We then assessed the localization of RAC and active RAC by immunostaining in these cells. Mammalian

RAC1 Ab staining, which cross-reacts with *Drosophila* RAC1 and 2 (catalog no. 23A8, Thermo Scientific), confirmed our WB findings because *RpS6*- and *pall* RNAi-treated S2 cells exhibited increased and decreased immunostainings, respectively, compared with mock-treated S2 cells (Figure S5A). To find out whether RAC levels resulted in similar active RAC levels in the cells, we also stained these RNAi-treated cells with a monoclonal Ab directed against active mammalian RAC1. This

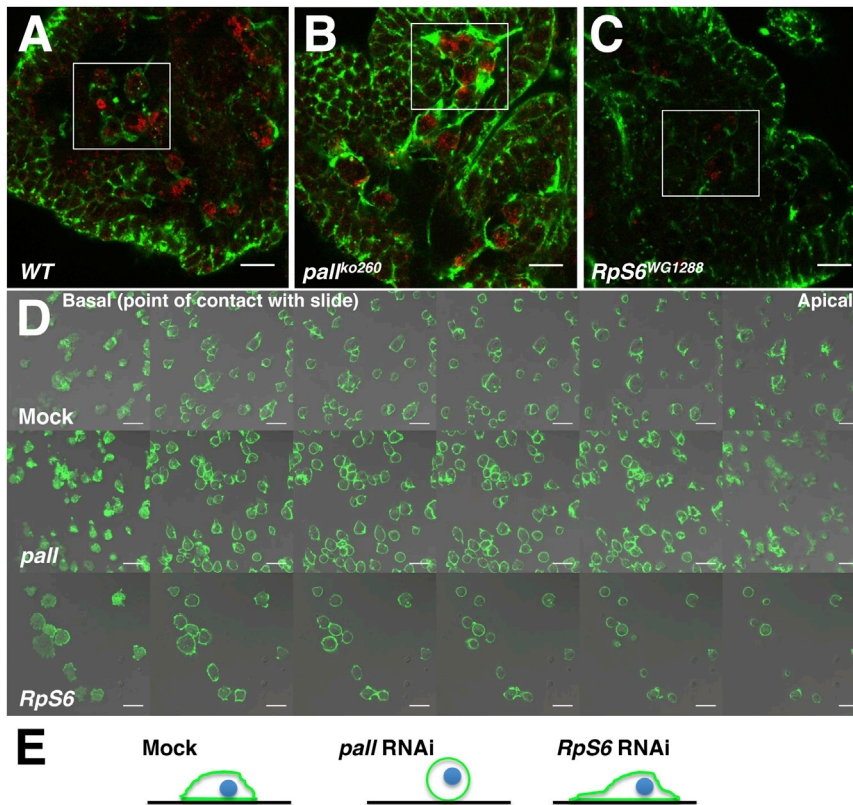


**Figure 5. PALL Promotes Actin Remodeling during AC Clearance**

(A–C) Confocal micrographs of Actin (green) and CRQ (red) immunostaining of *yw* embryos (wild-type [WT] control in [A]), *pall*<sup>ko260</sup> (B), and *RpS6*<sup>WG1288</sup> (C) mutant embryos.

(D) Confocal micrographs of mock-treated, *pall* RNAi, or *RpS6* RNAi S2 cells stained with phalloidin. z stack images through the cells were collected 1.74  $\mu\text{m}$  apart (the basal membrane is in contact with the glass slide). Scale bars, 10  $\mu\text{m}$ . (E) Schematic summarizing F-actin staining (green) distribution and cell shape for mock-treated and *pall* and *RpS6* RNAi S2 cells seen in (D). Green lines and blue circles represent actin and nuclei, respectively. Black lines represent the slides.

See also Figure S4.

*Pectobacterium carotovorum* (also known as *Erwinia carotovora* 15 [Ecc15]) and Gram-positive *Enterococcus faecalis* (*Ef*) (Figure S6A), as well as their bacterial loads (Figure S6B), were similar in *pall*<sup>ko</sup> mutant flies and control flies. Injections of Alexa 488 (green) *Escherichia coli* in *pall*<sup>ko</sup> (Figure S6C') and their control flies (Figure S6C) or of Alexa 488 *Staphylococcus aureus* (data not shown) or their pH-sensitive pHrodo-red equivalent

Ab cross-reacted with *Drosophila* RAC2 specifically (Figure S5B) and labeled the membranes of all treated cells. Again, *pall*- and *RpS6* RNAi-treated S2 cells showed reduced and increased staining, respectively, compared with mock-treated S2 cells (Figure 6C). We then asked whether we could rescue the phagocytosis defect of *pall* by overexpressing the *Drosophila* UAS-*Rac2* transgene in the *pall*<sup>ko</sup> mutant under the control of the macrophage-specific *crq-gal4* driver. As previously for *pall*<sup>ko</sup>, *crq-gal4;pall*<sup>ko</sup> homozygous macrophages had a significantly diminished PI of  $1.44 \pm 0.12$  compared with UAS-*Rac2*/+; *crq-gal4*/+; *pall*<sup>ko</sup>/+ heterozygous control macrophages (PI =  $2.41 \pm 0.13$ ,  $p < 0.001$ ), whereas *pall*<sup>ko</sup> rescue macrophages that overexpressed UAS-*Rac2* under the control of *crq-gal4* (UAS-*Rac2*/+; *crq-gal4*/+; *pall*<sup>ko</sup>) had a PI of  $2.09 \pm 0.19$ , which was statistically significantly rescued compared with that of *crq-gal4;pall*<sup>ko</sup> homozygous macrophages ( $p = 0.01$ ) but not statistically different from the UAS-*Rac2*/+; *crq-gal4*/+; *pall*<sup>ko</sup>/+ heterozygous control ( $p = 0.3$ ) (Figure 6D; Figures S5C–S5E). Therefore, PALL allows for the degradation of RpS6 via the proteasome that leads to the upregulation and activation of RAC2 and F-actin rearrangement to promote efferocytosis in vivo.

#### Nuclear Translocation of PALL in Response to ACs Confers Its Phagocytic Specificity

Considering the role of PALL upstream of RAC2 activation in efferocytosis, and because bacteria are cleared by *Drosophila* hemocytes via RAC2-mediated phagocytosis (Avet-Rochex et al., 2007), we next asked whether *pall*<sup>ko</sup> mutants were susceptible to infection. Survival rates of Gram-negative

(data not shown; Figures S6D and S6D') did not reveal any defect in their uptake (Figures S6C and S6C') or in their phagosomal degradation (Figures S6D and S6D'). The *pall*<sup>ko</sup> flies survived *E. coli* (Figure S6E) and *S. aureus* (Figure S6F) septic injuries equally well as their controls, and the loss of *pall* did not exacerbate the phenotype of mutant flies of the IMD pathway that are susceptible to a low dose of infection by *E. coli* (Figure S6E). Therefore, *pall* is not required for bacteria killing or phagocytosis and plays a specific role in efferocytosis.

Having found previously that ACs regulate the expression level of CRQ, which localizes at the phagosomal membranes during AC clearance and participates in efferocytosis (Franc et al., 1996, 1999), we asked whether ACs could regulate PALL expression and/or its localization. PALL has two potential nuclear export signals (NESs) at its amino acids L6 and L10, as predicted by the NetNES 1.1 server (la Cour et al., 2004; Figure S6G). We independently expressed in S2 cells a wild-type HA-tagged PALL (HA-PALLFL; Figure S6H; Movie S1) and versions of PALL in which the leucines of its NES were mutated into alanines (HA-NESPALL; Figure S6H; Movie S2) or in which the NES was replaced by a nuclear localization signal (NLS) (HA-NLSPALL; Figure S6H; Movie S3). After staining these cells with a HA Ab and either DAPI or DRAQ5 DNA dyes, we found that both HA-NESPALL (Figure 7B) and HA-NLSPALL (Figure 7C) were strictly localized to the nuclei of all transfected S2 cells as anticipated. However, although HA-PALLFL was expressed in the nuclei of most transfected S2 cells, it was also found to localize both in the nuclei and cytoplasm of all transfected S2 cells that were bound to/engulfing and/or had fully ingested ACs (Figure 7A;

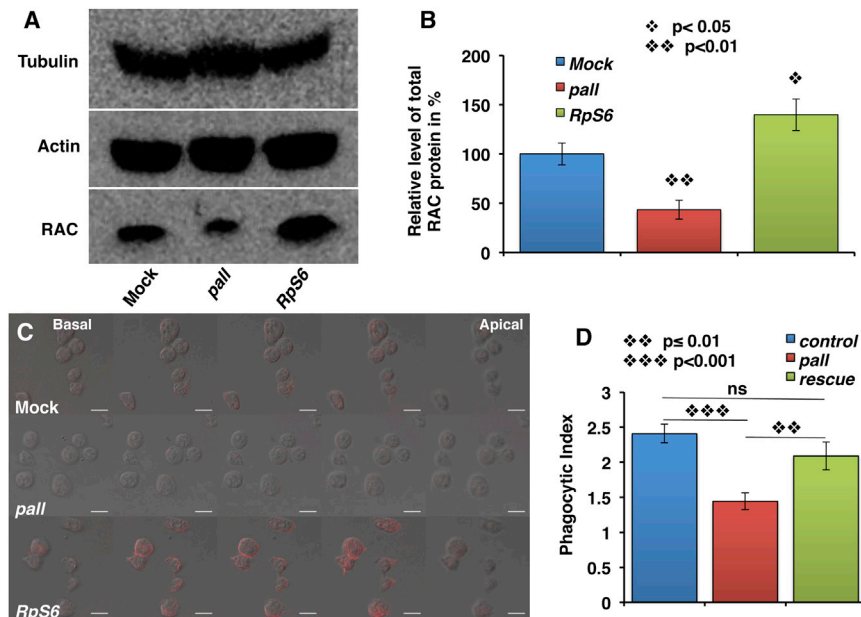


### Figure 6. RpS6 Targeting by PALL Promotes RAC Upregulation and Activation

(A) WB of protein extracts from mock-treated, *pall* RNAi, or *RpS6* RNAi S2 cells probed with tubulin and monomeric actin (internal controls) and mammalian RAC1 Abs.

(B) Graph showing the percent  $\pm$  SEM of RAC protein expression in *pall* and *RpS6* RNAi S2 cells relative to mock-treated cells (control normalized at 100%) based on three separate experiments.

(C) Confocal micrographs of mock-treated, *pall* RNAi, and *RpS6* RNAi S2 cells stained with active RAC Ab. z stack images through the cells were collected at 1.74  $\mu$ m intervals. Scale bars, 10  $\mu$ m.

(D) Graph showing the mean PIs  $\pm$  SEM of *crq-gal4* control, *crq-gal4;pallko* mutant, and *pall<sup>ko</sup>* macrophages that overexpress *UAS-Rac2* under the control of *crq-gal4*. ns, not significant.

See also Figure S5.

Movie S1). In contrast, mutated HA-NESPALL never translocated, even when these cells engulfed endogenous ACs (white arrow, Figure 7B; Movie S2; of note is that endogenous PALL is present in these cells), and neither did mutated HA-NLSPALL (Figure 7C; Movie S3). Moreover, HA-PALLFL remained nuclear in S2 cells that had bound or fully ingested Gram-negative (*E. coli*) or Gram-positive (*S. aureus*) bacteria (Figure 7F). Therefore, the NES is required for the translocation of PALL from the nuclei to the cytoplasm of S2 cells in response to ACs, and this translocation is dependent on the binding/recognition of ACs (Figures 7D and 7E). These results demonstrate that ACs play an active role in regulating PALL localization that promotes efferocytosis and confers PALL its specificity in this process.

## DISCUSSION

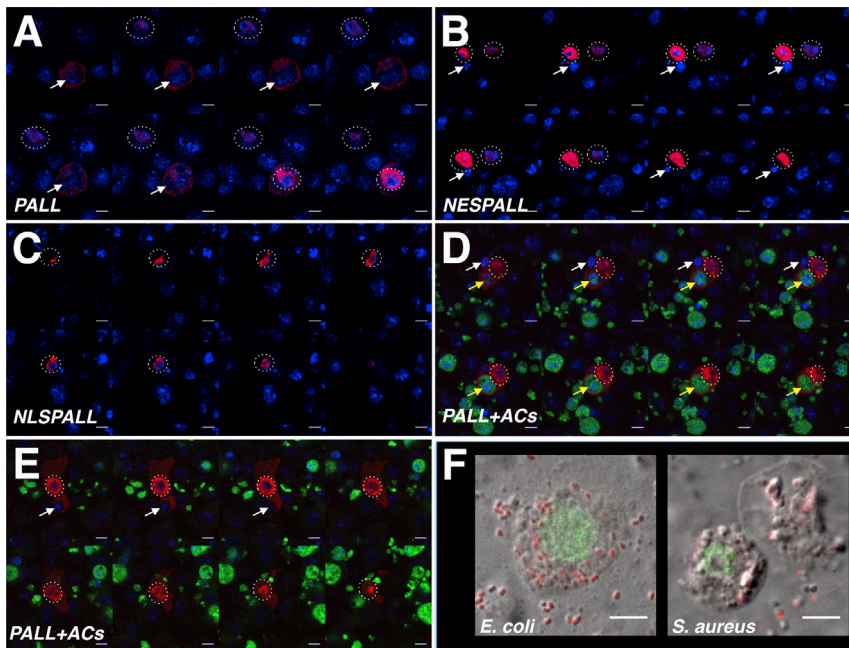
The PALL-SCF complex and proteasomal degradation are required for efficient AC engulfment (Silva et al., 2007). However, it was not clear how this promoted efferocytosis. Here we provide insights into the molecular mechanisms by which PALL promotes efferocytosis. Upon recognition and binding of ACs, PALL translocates from the nucleus to the cytoplasm, where it forms a PALL-SCF complex and specifically interacts with and targets phosphorylated RpS6 to polyubiquitylation and degradation via the 26S proteasome, which results in an increased level and activity of RAC2, followed by actin remodeling to promote efferocytosis.

RpS6, a component of the small 40S subunit of the ribosome, has highly conserved serines that are phosphorylated by S6 and RSK kinases following a wide variety of stimuli (Meyuhas, 2008). RpS6 has long been thought to be required for various functions, including global protein synthesis, the translation of mRNAs containing a 5' terminal oligopyrimidine tract (TOP mRNAs), cell size and proliferation, and glucose homeostasis (Meyuhas, 2008). However, *RpS6<sup>P-/-</sup>* knockin mice in which all five serines of RpS6 were mutated into alanines show a 2.5-fold increase

(Ruvinsky et al., 2005). *RpS6<sup>P-/-</sup>* mice have similar weights as wild-type mice, although some of their cells are small because of impaired growth as they undergo compensatory proliferation (Ruvinsky et al., 2005). *RpS6<sup>P-/-</sup>* mice also have reduced glucose disposal capacity because of a 2-fold reduction in the secretion of circulating and pancreatic insulin by small  $\beta$  cells (Ruvinsky et al., 2005). In at least one study, intravenous injection of mice with rat breast carcinoma cells resulted in poorly phagocytic alveolar macrophages with reduced cell-autonomous glucose oxidation that led to tumor metastasis (Gudewicz and Saba, 1977). It will be interesting to find out whether reduced glucose oxidation in these alveolar macrophages correlates with reduced glucose homeostasis because of defective RpS6 regulation.

*Drosophila* RpS6 appears to play immune-specific roles because *RpS6* mutants have overgrown lymph glands (the larval hematopoietic organs), abnormal proliferation and differentiation of enlarged hemocytes, and melanotic masses caused by erroneous encapsulation of larval tissues (Stewart and Denell, 1993; Watson et al., 1992). These phenotypes suggest that losing RpS6 results in hemocyte hyperactivation. This is consistent with our data showing that *RpS6*-RNAi S2 cells are more phagocytic. We did not, however, observe any increased efferocytosis by macrophages in *RpS6* mutant embryos in vivo. This is likely due to the limited amount of ACs present in the embryo compared with the excess of ACs used in our S2 cell assay. Although RpS6 acts as a negative regulator of efferocytosis, other proteins of the ribosome small subunit, including RpS2 and RpS10b, do not participate in this process because RNAi in S2 cells or in vivo overexpression experiments did not reveal any significant effect on efferocytosis (Figure S3). Yet another ribosomal protein, RpS17, appears to act as a positive regulator of efferocytosis because RNAi for *RpS17* in S2 cells results in these cells being less efficient at engulfing ACs (H.X. and N.C.F., unpublished data). Further experiments will be required to determine the precise role of RpS17 in AC clearance.





(F) Nuclear localization of PALL on confocal micrographs of HA Ab-stained (green) HA-PALLFL-expressing S2 cells that have engulfed *E. coli* and *S. aureus* bacteria.

Scale bars, 5  $\mu$ m. See also Figure S6.

### Figure 7. Regulation of PALL Localization by ACs Confers Its Specificity to Efferocytosis

(A–E) Z stack confocal images through DRAQ5- (A–C) or DAPI- (D–E) (blue) and HA Ab-double-stained (red) S2 cells expressing various forms of PALL.

(A) A HA-PALLFL expressing S2 cell that has engulfed an endogenous AC (white arrows) shows both nuclear (dotted circles surrounding the cell nuclei of interest) and cytoplasm HA-PALLFL protein expression, whereas a cell that has not engulfed nor bound to AC shows HA-PALLFL strictly in its nucleus.

(B) HA-NESPALL-expressing S2 cells where the leucine residues of the NES of PALL were mutated into alanines, which prevents PALL nuclear export even when cells have engulfed endogenous ACs. (C) HA-NLSPALL expressing S2 cells where the NES was replaced by a NLS show its nuclear localization.

(D and E) A HA-PALLFL expressing S2 cell that has engulfed an endogenous AC (white arrow) and a FITC-labeled AC (yellow arrow) (D) and a HA-PALLFL-expressing S2 cell that is engulfing an endogenous AC (white arrow) (E) showing both nuclear (dotted circle around the nucleus) and cytoplasmic localization of HA-PALLFL.

However, based on these experiments, we propose that RpS6 acts in efferocytosis independently of its ribosomal function. Interestingly, mammalian RpS6 can interact with proteins outside of the ribosome, including heat shock protein 90, alpha-virus nonstructural protein, and the death-associated protein kinase (Meyuhas, 2008), and is likely to also have functions that are independent of the translational machinery.

The nuclear export of PALL in response to ACs, but not to bacteria, is particularly important because it confers a specific role for RpS6 in efferocytosis. Indeed, *RpS6* RNAi in S2 cells results in an increase in phagocytosis of the Gram-positive bacterium *L. monocytogenes* (Agaisse et al., 2005), although the specific role of RpS6 in this system is not yet known. We carried out similar *RpS6* RNAi in S2 cells with new validation amplicons that have no target effects and exposed those S2 cells to fluorescent *E. coli* and *S. aureus* bacteria. We also found that knocking down *RpS6* enhanced phagocytosis of both *E. coli* and *S. aureus* (H.X. and N.C.F., unpublished data). Therefore, RpS6 acts as a negative regulator of bacterial clearance, although the mechanism by which RpS6 is regulated during this process is not known. Finally, *RpS6* RNAi in S2 cells also confers tolerance to *Drosophila* C virus infection, although it does so by acting in the context of its ribosomal function together with other ribosomal proteins (Cherry et al., 2005). Therefore, RpS6 can play many roles in *Drosophila* immunity, either directly or indirectly, via its ribosomal function or more specific functions that merit further investigation.

Phosphorylated RpS6 regulates F-actin organization and junctional protein recruitment at the blood-testis barrier during spermatogenesis, where increased levels of phosphorylated RpS6 disrupt the barrier and colocalize with disorganized F-actin

(Mok et al., 2012). F-actin rearrangement in phagocytosis is regulated by small GTPases of the RAC family. Our results demonstrate a negative role for *Drosophila* RpS6 in AC clearance and that proteasomal degradation of phosphorylated RpS6 by PALL-SCF leads to F-actin remodeling via the upregulation and activation of RAC2. RAC2 is the only GTPase required for efferocytosis in S2 cells (Cuttell et al., 2008), and overexpressing RAC2 in *pal*<sup>ko</sup> mutant macrophages rescued their phagocytosis defect, therefore linking PALL and RAC2 functions in vivo. Of further note, myoblasts of *RpS6*<sup>P-/P-</sup> mice have less contractile proteins, including myosins (Ruvinsky et al., 2009), suggesting that phosphorylation of RpS6 (and perhaps its degradation) is required to regulate myosin expression. Together, these observations further argue in favor of a role for RpS6 in the regulation of specific proteins in both mouse and *Drosophila* rather than a role in global protein synthesis. Whether RpS6 phosphorylation and proteasomal degradation in *Drosophila* macrophages or in other cells result in increased levels of proteins other than RAC2 to promote efferocytosis or other RpS6-mediated functions will need further investigation.

How the degradation of phosphorylated RpS6 results in higher levels and activation of RAC2 remains to be determined. Recent studies, however, have highlighted a role for specific E3 ligases, including SCF<sup>FBXL19</sup> and HACE1, in regulating mammalian RAC1 protein levels in cell migration and tumorigenesis (Torrino et al., 2011; Zhao et al., 2013). The small GTPase RhoA is also regulated by SCF<sup>FBXL19</sup> as well as by another E3 ubiquitin ligase, Smurf1, in cell migration (Wei et al., 2013). In this instance, Synaptopodin, an actin-associated protein, can compete with Smurf1 for binding to RhoA, thereby preventing its degradation (Asanuma et al., 2006). One possibility is that the accumulation

in the *pall* mutant of phosphorylated RpS6 may displace such an inhibitory protein, thereby allowing a specific E3-ubiquitin ligase to bind to and target RAC2 to polyubiquitylation and proteasomal degradation. In contrast, in a wild-type context, the PALL-SCF-mediated ubiquitylation and degradation of phosphorylated RpS6 may prevent the polyubiquitylation and degradation of RAC2 by allowing binding of a specific inhibitory protein to the RAC2-specific E3-ubiquitin ligase, resulting in elevated levels and activity of RAC2. Of note is that Smurf1 can also regulate a guanine nucleotide exchange factor (GEF) for yet another small GTPase, CDC42 (Yamaguchi et al., 2008). Therefore, the regulation of RpS6 may also lead to activation of RAC2 by indirectly regulating RAC2-specific GEFs or GAPs.

Future studies of the role of *Drosophila* RpS6 and the regulation of its phosphorylation and levels are likely to provide new insights into the role and regulation of mammalian RpS6 that may have implications for the development of treatments to fight autoimmune and neurodegenerative diseases. Moreover, high levels of phosphorylated RpS6 correlate with tumor progression and shorter survival prognostics in patients with esophageal squamous cell carcinoma (Chaisuparat et al., 2013). Whether RpS6 plays a role in AC clearance in mammals remains to be determined, but a lack of engulfment of cancer cells by poorly phagocytic macrophages with high levels of phosphorylated RpS6 may favor the development of this cancer. Therefore, a better understanding of the phosphorylation and regulation of RpS6 levels and its role in phagocytosis will likely provide us with drug targets to fight cancer progression.

## EXPERIMENTAL PROCEDURES

### Fly Strains

Most fly stocks were from the Bloomington *Drosophila* stock center. RpS6<sup>WG1288</sup> and S6klf<sup>gn-458-1</sup> flies were provided by Leonie M. Quinn (University of Melbourne) and by F. Rob Jackson (Tufts University School of Medicine), respectively. UAS transgenic fly lines were generated at BestGene or supplied by FLYORF. Fly stocks were maintained at 25°C in Superfly incubators (Genesee) on standard medium. For plasmid constructs, see Supplemental Experimental Procedures.

### Generation of HA-PALLFL, HA-PALLΔF, and HA-SLIMB Stable S2 Cell Lines

S2 cells were transfected with Effectene (QIAGEN) according to the supplier's protocol using 950 ng of HA-PALLFL, HA-PALLΔF, or HA-SLIMB (N terminus-tagged constructs in the pMT-N-3xHA tag vector) DNA and 50 ng of pHygro vector DNA. Cells were resuspended in complete medium with 300 μg/ml of Hygromycin B to select clones that had integrated pHygro DNA. Clones were tested for integration of pMT constructs and expression of HA-tagged proteins by WB following standard protocols after treating the cells with 0.7 mM of CuSO<sub>4</sub> to induce expression under the control of the MT promoter.

### Immunoprecipitations and Tandem MS Analysis

PALL, PALLΔF, or SLIMB expression was induced with 0.7 mM CuSO<sub>4</sub>. Cells were treated with 25 μM MG132 for 6 hr (Sigma), harvested at 48 and 72 hr post-CuSO<sub>4</sub> treatment, and lysed in 50 mM Tris HCl (pH 7.4), 150 mM NaCl, 1 mM EDTA, and 1% NP40 with Complete EDTA-free protease inhibitor (Roche). Lysates were centrifuged at 10,000 × *g* for 30 min, and supernatants were added to EZ view HA beads (Sigma) overnight at 4°C. After several washes, proteins were eluted in 0.2 M Glycine (pH 2.5) and neutralized with ammonium bicarbonate. Impurities removed by trichloro-acetic acid precipitation, and samples were subjected to tandem MS analysis (Supplemental Experimental Procedures).

### Transient Transfections and Immunoprecipitations

S2 cells were transfected with Effectene (QIAGEN) according to the supplier's protocol. Expression of tagged versions of RpS6, PALL, and SkpA were induced with CuSO<sub>4</sub> at 24 hr, and the cells were harvested and lysed at 48–72 hr after transfection. Lysates were centrifuged at 10,000 × *g* for 30 min, and supernatants were incubated with EZ view HA beads or anti-V5 agarose affinity gel (Sigma). Purified samples were resolved by 4%–15% gradient SDS-PAGE (Bio-Rad). In WBs, Abs were used at the following dilutions: rat anti-HA (Roche) and mouse anti-FLAG (Sigma), 1:2,000; mouse anti-V5 (Invitrogen), 1:5,000. Anti-rat or anti-mouse horseradish peroxidase (HRP)-coupled secondary Abs (Jackson ImmunoResearch Laboratories) were used at a 1:10,000 dilution, followed by ECL detection following the supplier's protocol (Pierce).

### Stability and Ubiquitylation Assays

For the stability assay, pAc5.1/V5-HisA-RpS6 was transiently transfected into the HA-PALLFL stable S2 cell line with Effectene (QIAGEN) according to the supplier's instructions. The cells were then treated with CuSO<sub>4</sub> at 24 hr post-transfection, followed by MG132 (Sigma) at a concentration of 50 μM for 4 hr. For the ubiquitylation assay, pAc5.1/V5-HisA-RpS6 and pAc5.1/UB were transiently transfected into the HA-PALLFL stable S2 cell line with Effectene (QIAGEN). PALL expression was induced with CuSO<sub>4</sub> at 24 hr posttransfection. The cells were then treated with MG132 (Sigma) at a concentration of 50 μM for 4 hr, lysed, and subjected to IPs and WBs as described above. The Ub (P4D1) mouse monoclonal Ab (Santa Cruz Biotechnology) was used at a 1:200 dilution.

The in vivo phagocytosis assay, phagocytosis index quantification, RNA interference, and S2 cell phagocytosis assays and their statistical analyses were performed as in Cuttell et al. (2008) and Silva et al. (2007).

### Statistical Analyses

Statistical *p* values were derived using ANOVA (for IPs) or Student's *t* test and are indicated in the text and figures.

### Ends-Out Gene Targeting

Donor targeting constructs were built by insertion of two 3 kb regions (upstream and downstream of the *pall* target gene) into two multiple cloning sites of the targeting vector pXH87. These constructs were then injected into *w<sup>1118</sup>* embryos using established methods to obtain transgenics (Bestgene). The ends-out gene targeting procedure was performed as described in Chen et al. (2009). To induce double-stranded DNA breaks, heat shock was performed at 38°C for 90 min on day 3 after egg-laying. Target gene-specific PCR amplification was performed using primers corresponding to a sequence within the *pall* gene to verify homozygous knockouts (no PCR product). *crq* primer sets were used as a control (Supplemental Experimental Procedures).

Actin staining and RAC immunostaining were performed according to standard protocols (Supplemental Experimental Procedures).

### RAC Quantification

RAC WBs were performed after 3 days of RNAi treatment of S2 cells as described above. Cells were lysed in 50 mM Tris HCl (pH 7.4), 0.1% SDS, 200 mM NaCl, 5 mM MgCl<sub>2</sub>, 1 mM dithiothreitol, 1% NP40, and 10% Glycerol with Complete EDTA-free protease inhibitor (Roche) and subjected to WBs. Mouse RAC1 monoclonal Ab (catalog no. 23A8, Thermo Scientific), mouse Actin Ab (catalog no. A-2066, Sigma), and rabbit α-tubulin Ab (catalog no. 11H10, Cell Signaling Technology) were used at 1:1,000. Secondary anti-Mouse HRP-coupled Abs (Jackson ImmunoResearch Laboratories) were used at 1:10,000, followed by ECL detection.

All experiments with vertebrate animals were performed at the Pocono Rabbit Farm and Laboratory in accordance with relevant institutional and national guidelines and regulations. An animal protocol (10-0013-2) was approved by the Institutional Animal Care and Use Committee of The Scripps Research Institute.

## SUPPLEMENTAL INFORMATION

Supplemental Information includes Supplemental Experimental Procedures, six figures, and three movies and can be found with this article online at <http://dx.doi.org/10.1016/j.devcel.2014.11.015>.

## AUTHOR CONTRIBUTIONS

H.X., H.W., E.S., J.T., A.G., N.B., and N.C.F. conceived, designed, and performed the experiments, analyzed and interpreted the data, and wrote the manuscript.

## ACKNOWLEDGMENTS

We thank Dr. Xun Huang (Institute of Genetics and Developmental Biology, Chinese Academy of Sciences, Beijing, China) for the pXH87 plasmid; Dr. Jin Jiang (UT Southwestern Medical Center, Dallas, TX) for the pUAST-UB construct; and Dr. Leonie M. Quinn (University of Melbourne, Parkville, Australia), Dr. F. Rob Jackson (Tufts University School of Medicine, Boston, MA), and the Bloomington Stock Center and FLYORF for fly strains. We also thank Claude Desplan, Sergio Grinstein, and Céline DerMardirossian for critically reading this manuscript and Céline DerMardirossian for valuable advice on RAC and actin stainings. The work was funded by a program leader-track grant from the Medical Research Council (to N.C.F.), by core support to the MRC Cell Biology Unit (to N.C.F. and E.A.S.), by an Irvington Institute postdoctoral fellowship of the Cancer Research Institute (to H.X.), by a TSRI-Advanced Discovery Institute grant provided by Novartis and NIH, National Institute of Allergy and Infectious Diseases Grant R01 AI093687-01A1 (to N.C.F.), and by Research Resource Grant P41 RR011823 of the NIH (to J.R.Y.). Stocks from the Bloomington *Drosophila* Stock Center (NIH P40OD018537) were used in this study.

Received: July 12, 2014

Revised: October 6, 2014

Accepted: November 10, 2014

Published: December 18, 2014

## REFERENCES

- Agaisse, H., Burrack, L.S., Phillips, J.A., Rubin, E.J., Perrimon, N., and Higgins, D.E. (2005). Genome-wide RNAi screen for host factors required for intracellular bacterial infection. *Science* *309*, 1248–1251.
- Allen, L.A., and Aderem, A. (1996). Mechanisms of phagocytosis. *Curr. Opin. Immunol.* *8*, 36–40.
- Asanuma, K., Yanagida-Asanuma, E., Faul, C., Tomino, Y., Kim, K., and Mundel, P. (2006). Synaptopodin orchestrates actin organization and cell motility via regulation of RhoA signalling. *Nat. Cell Biol.* *8*, 485–491.
- Avet-Rochex, A., Perrin, J., Bergeret, E., and Fauvarque, M.O. (2007). Rac2 is a major actor of *Drosophila* resistance to *Pseudomonas aeruginosa* acting in phagocytic cells. *Genes Cells* *12*, 1193–1204.
- Brown, E.J. (1995). Phagocytosis. *BioEssays* *17*, 109–117.
- Chaisuparat, R., Rojanawatsirivej, S., and Yodsanga, S. (2013). Ribosomal protein S6 phosphorylation is associated with epithelial dysplasia and squamous cell carcinoma of the oral cavity. *Pathol. Oncol. Res.* *19*, 189–193.
- Chen, H., Ma, Z., Liu, Z., Tian, Y., Xiang, Y., Wang, C., Scott, M.P., and Huang, X. (2009). Case studies of ends-out gene targeting in *Drosophila*. *Genesis* *47*, 305–308.
- Cherry, S., Doukas, T., Armknecht, S., Whelan, S., Wang, H., Sarnow, P., and Perrimon, N. (2005). Genome-wide RNAi screen reveals a specific sensitivity of IRES-containing RNA viruses to host translation inhibition. *Genes Dev.* *19*, 445–452.
- Cuttell, L., Vaughan, A., Silva, E., Escaron, C.J., Lavine, M., Van Goethem, E., Eid, J.P., Quirin, M., and Franc, N.C. (2008). Undertaker, a *Drosophila* Junctophilin, links Draper-mediated phagocytosis and calcium homeostasis. *Cell* *135*, 524–534.
- Deshaies, R.J. (1999). SCF and Cullin/Ring H2-based ubiquitin ligases. *Annu. Rev. Cell Dev. Biol.* *15*, 435–467.
- Ferrandon, D., Imler, J.L., Hetru, C., and Hoffmann, J.A. (2007). The *Drosophila* systemic immune response: sensing and signalling during bacterial and fungal infections. *Nat. Rev. Immunol.* *7*, 862–874.
- Finnemann, S.C., Leung, L.W., and Rodriguez-Boulan, E. (2002). The lipofuscin component A2E selectively inhibits phagolysosomal degradation of photoreceptor phospholipid by the retinal pigment epithelium. *Proc. Natl. Acad. Sci. USA* *99*, 3842–3847.
- Franc, N.C., Dimarcq, J.L., Lagueux, M., Hoffmann, J., and Ezekowitz, R.A. (1996). Croquemort, a novel *Drosophila* hemocyte/macrophage receptor that recognizes apoptotic cells. *Immunity* *4*, 431–443.
- Franc, N.C., Heitzler, P., Ezekowitz, R.A., and White, K. (1999). Requirement for croquemort in phagocytosis of apoptotic cells in *Drosophila*. *Science* *284*, 1991–1994.
- Fuller, A.D., and Van Eldik, L.J. (2008). MFG-E8 regulates microglial phagocytosis of apoptotic neurons. *J. Neuroimmune Pharmacol.* *3*, 246–256.
- Gudewicz, P.W., and Saba, T.M. (1977). Inhibition of phagocytosis and glucose metabolism of alveolar macrophages during pulmonary tumour growth. *Br. J. Cancer* *36*, 670–677.
- Gumienny, T.L., Brugnera, E., Tosello-Tramont, A.C., Kinchen, J.M., Haney, L.B., Nishiwaki, K., Walk, S.F., Nemergut, M.E., Macara, I.G., Francis, R., et al. (2001). CED-12/ELMO, a novel member of the Crkl/Dock180/Rac pathway, is required for phagocytosis and cell migration. *Cell* *107*, 27–41.
- Han, C.Z., and Ravichandran, K.S. (2011). Metabolic connections during apoptotic cell engulfment. *Cell* *147*, 1442–1445.
- Hanayama, R., Miyasaka, K., Nakaya, M., and Nagata, S. (2006). MFG-E8-dependent clearance of apoptotic cells, and autoimmunity caused by its failure. *Curr. Dir. Autoimmun.* *9*, 162–172.
- Henson, P.M., Bratton, D.L., and Fadok, V.A. (2001). Apoptotic cell removal. *Curr. Biol.* *11*, R795–R805.
- Khush, R.S., Cornwell, W.D., Uram, J.N., and Lemaitre, B. (2002). A ubiquitin-proteasome pathway represses the *Drosophila* immune deficiency signaling cascade. *Curr. Biol.* *12*, 1728–1737.
- Kinchen, J.M., Cabello, J., Klingele, D., Wong, K., Feichtinger, R., Schnabel, H., Schnabel, R., and Hengartner, M.O. (2005). Two pathways converge at CED-10 to mediate actin rearrangement and corpse removal in *C. elegans*. *Nature* *434*, 93–99.
- la Cour, T., Kiemer, L., Mølgaard, A., Gupta, R., Skriver, K., and Brunak, S. (2004). Analysis and prediction of leucine-rich nuclear export signals. *Protein Eng. Des. Sel.* *17*, 527–536.
- Meyuhas, O. (2008). Physiological roles of ribosomal protein S6: one of its kind. *Int. Rev. Cell. Mol. Biol.* *268*, 1–37.
- Modlin, R.L. (2012). Innate immunity: ignored for decades, but not forgotten. *J. Invest. Dermatol.* *132*, 882–886.
- Mok, K.W., Mruk, D.D., Silvestrini, B., and Cheng, C.Y. (2012). rpS6 Regulates blood-testis barrier dynamics by affecting F-actin organization and protein recruitment. *Endocrinology* *153*, 5036–5048.
- Muñoz, L.E., Janko, C., Schulze, C., Schorn, C., Sarter, K., Schett, G., and Herrmann, M. (2010). Autoimmunity and chronic inflammation - two clearance-related steps in the etiopathogenesis of SLE. *Autoimmun. Rev.* *10*, 38–42.
- Radimerski, T., Mini, T., Schneider, U., Wettenhall, R.E., Thomas, G., and Jenö, P. (2000). Identification of insulin-induced sites of ribosomal protein S6 phosphorylation in *Drosophila melanogaster*. *Biochemistry* *39*, 5766–5774.
- Ruvinsky, I., Sharon, N., Lerer, T., Cohen, H., Stolovich-Rain, M., Nir, T., Dor, Y., Zisman, P., and Meyuhas, O. (2005). Ribosomal protein S6 phosphorylation is a determinant of cell size and glucose homeostasis. *Genes Dev.* *19*, 2199–2211.
- Ruvinsky, I., Katz, M., Dreazen, A., Gielchinsky, Y., Saada, A., Freedman, N., Mishani, E., Zimmerman, G., Kasir, J., and Meyuhas, O. (2009). Mice deficient in ribosomal protein S6 phosphorylation suffer from muscle weakness that reflects a growth defect and energy deficit. *PLoS ONE* *4*, e5618.
- Schneider, I. (1972). Cell lines derived from late embryonic stages of *Drosophila melanogaster*. *J. Embryol. Exp. Morphol.* *27*, 353–365.
- Shishido, S.N., Varahan, S., Yuan, K., Li, X., and Fleming, S.D. (2012). Humoral innate immune response and disease. *Clin. Immunol.* *144*, 142–158.
- Silva, E., Au-Yeung, H.W., Van Goethem, E., Burden, J., and Franc, N.C. (2007). Requirement for a *Drosophila* E3-ubiquitin ligase in phagocytosis of apoptotic cells. *Immunity* *27*, 585–596.

- Stewart, M.J., and Denell, R. (1993). Mutations in the *Drosophila* gene encoding ribosomal protein S6 cause tissue overgrowth. *Mol. Cell. Biol.* *13*, 2524–2535.
- Tepass, U., Fessler, L.I., Aziz, A., and Hartenstein, V. (1994). Embryonic origin of hemocytes and their relationship to cell death in *Drosophila*. *Development* *120*, 1829–1837.
- Torrino, S., Visvikis, O., Doye, A., Boyer, L., Stefani, C., Munro, P., Bertoglio, J., Gacon, G., Mettouchi, A., and Lemichez, E. (2011). The E3 ubiquitin-ligase HACE1 catalyzes the ubiquitylation of active Rac1. *Dev. Cell* *21*, 959–965.
- Watson, K.L., Konrad, K.D., Woods, D.F., and Bryant, P.J. (1992). *Drosophila* homolog of the human S6 ribosomal protein is required for tumor suppression in the hematopoietic system. *Proc. Natl. Acad. Sci. USA* *89*, 11302–11306.
- Wei, J., Mialki, R.K., Dong, S., Khoo, A., Mallampalli, R.K., Zhao, Y., and Zhao, J. (2013). A new mechanism of RhoA ubiquitination and degradation: roles of SCF(FBXL19) E3 ligase and Erk2. *Biochim. Biophys. Acta* *1833*, 2757–2764.
- Yamaguchi, K., Ohara, O., Ando, A., and Nagase, T. (2008). Smurf1 directly targets hPEM-2, a GEF for Cdc42, via a novel combination of protein interaction modules in the ubiquitin-proteasome pathway. *Biol. Chem.* *389*, 405–413.
- Zhao, J., Mialki, R.K., Wei, J., Coon, T.A., Zou, C., Chen, B.B., Mallampalli, R.K., and Zhao, Y. (2013). SCF E3 ligase F box protein complex SCF(FBXL19) regulates cell migration by mediating Rac1 ubiquitination and degradation. *FASEB J.* *27*, 2611–2619.